Cell Reports, Volume *35*

Supplemental information

Immune checkpoint blockade reprograms systemic immune landscape and tumor microenvironment in obesity-associated breast cancer

Ajeeth K. Pingili, Mehdi Chaib, Laura M. Sipe, Emily J. Miller, Bin Teng, Rahul Sharma, Johnathan R. Yarbro, Sarah Asemota, Qusai Al Abdallah, Tahliyah S. Mims, Tony N. Marion, Deidre Daria, Radhika Sekhri, Alina M. Hamilton, Melissa A. Troester, Heejoon Jo, Hyo Young Choi, D. Neil Hayes, Katherine L. Cook, Ramesh Narayanan, Joseph F. Pierre, and Liza Makowski

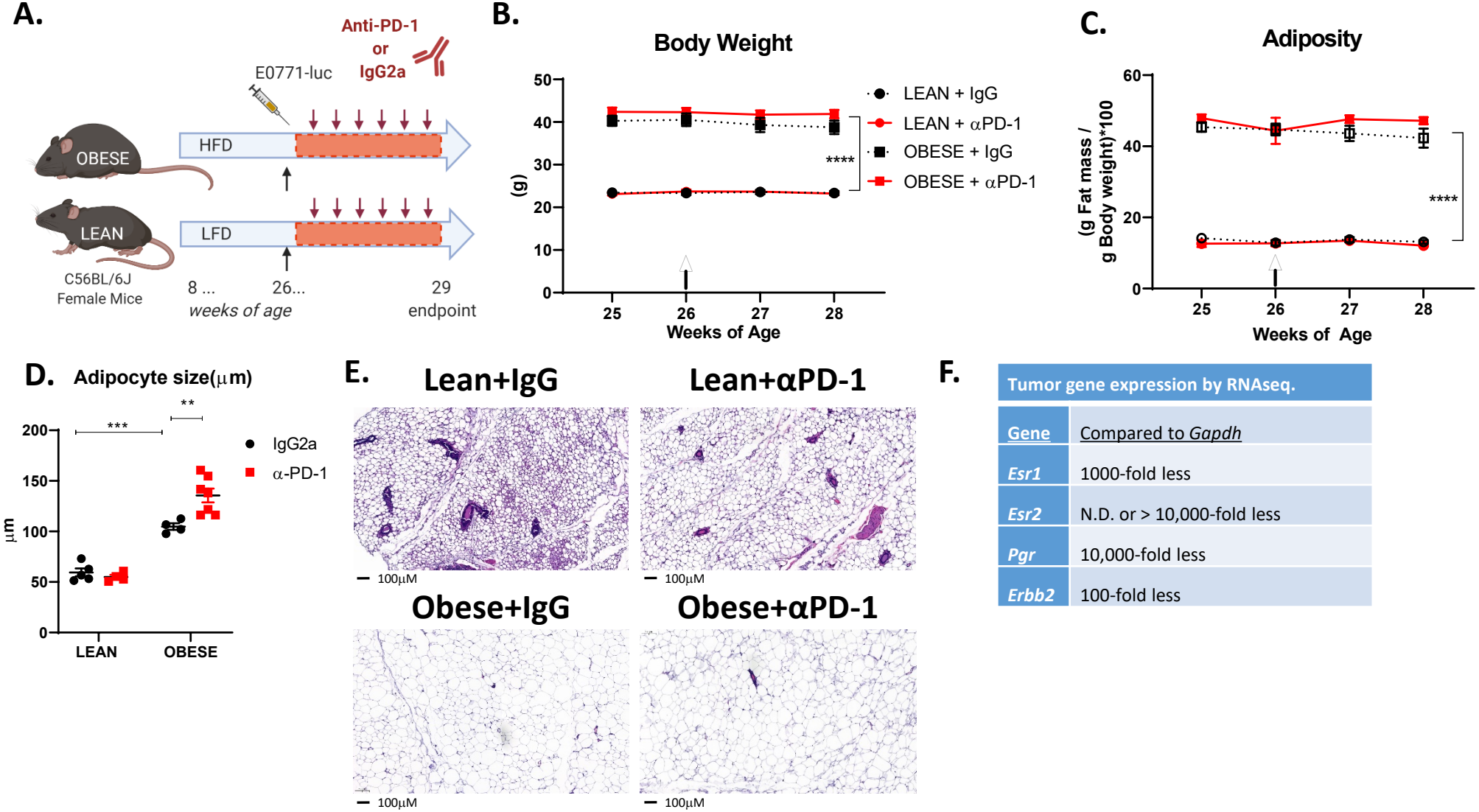

F.

Tumor gene expression by RNAseq.	
Gene	Compared to *Gapdh*
Esr1	1000-fold less
Esr2	N.D. or > 10,000-fold less
Pgr	10,000-fold less
Erbb2	100-fold less

Supplemental Figure 1. Establishment of obesity model to determine the impact of immune checkpoint inhibition in breast cancer. A. Study design schematic: C57BL/6J female mice were started on a low fat diet (LFD, lean) or high fat diet (HFD, obese) at 8 weeks of age and maintained on diet throughout the study. Mice were injected in the 4th mammary gland with 250 X 10^5 E0771-luciferase (luc) cells in 25% matrigel (black arrow) at 26 weeks of age after 18 weeks on diets. Three days post tumor cell injection, control IgG2a or anti-PD-1 antibody (200ug in 50μl/mouse i.p., red boxes) was injected every 3 days until endpoint sacrifice at 29 weeks of age (red arrows). N=8-9/lean and N=11-12/obese per intervention group. **B.** Body weights were recorded 1 week before injection of cells and weekly during tumor progression. **C.** Adiposity was measured by EchoMRI. Data are shown as mean ± SEM. **** P<0.0001 for Lean vs. Obese in IgG2a controls and anti-PD-1 for all time points. Statistics were calculated using 2-way ANOVA with repeated measures and Tukey post-hoc test in GraphPad Prism. **D.** Adipocyte diameter was measured in H&E sections using Case Viewer in 6 high power fields. **E.** Representative images of adipose tissue is shown (10X). **F.** Expression of receptors for ERα (*Esr1*), ERβ (*Esr2*), PG (*Pgr*), and HER2 (*Erbb2*) relative to *Gapdh* by RNA-seq of obese tumors. Relates to Figures 1 and 2.

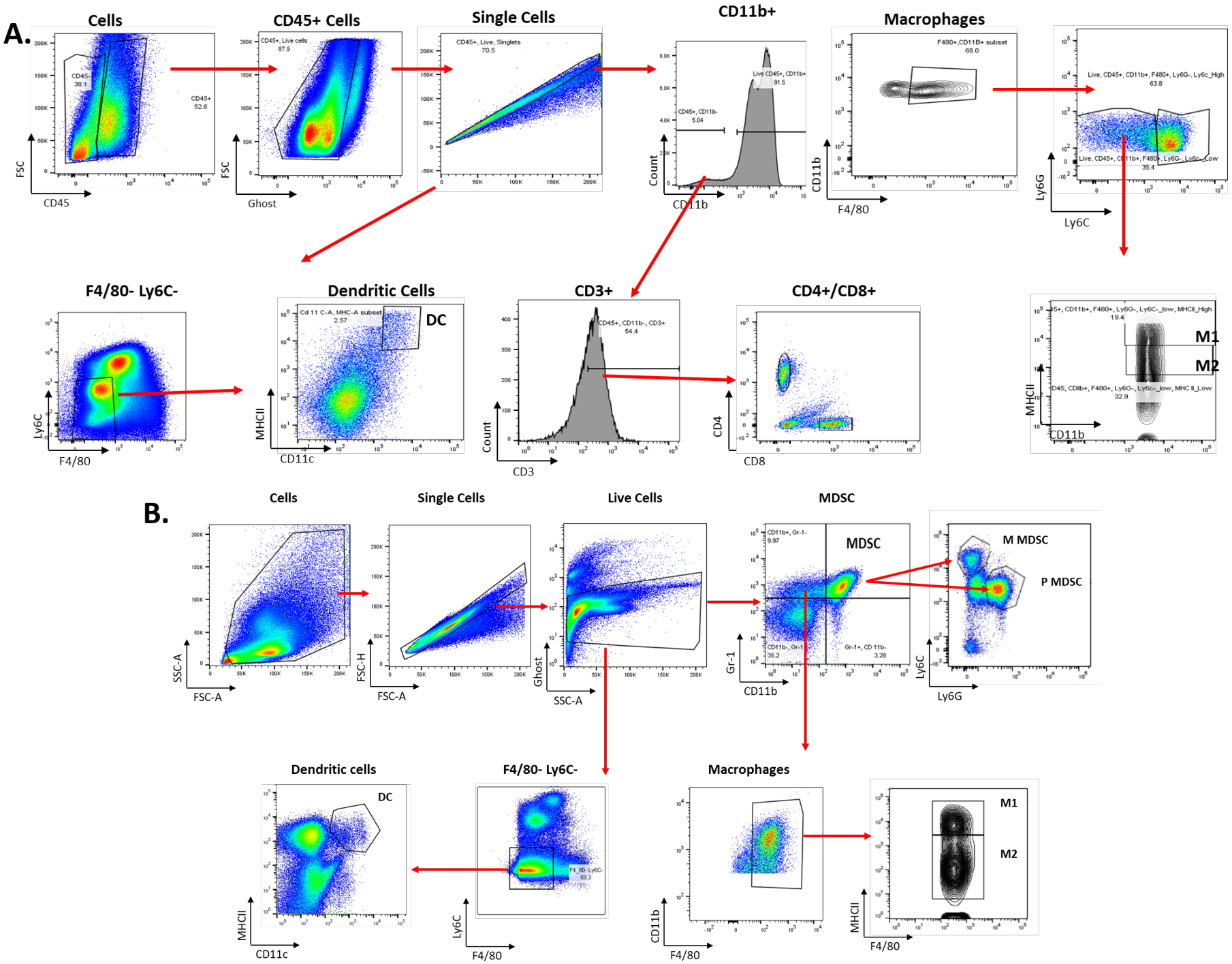

Supplemental Figure 2. Gating scheme for flow cytometry analysis of immune cells in tumor or bone marrow and spleen single cell suspension. (**A**) Total immune cells in the TME were gated by plotting forward scatter area versus CD45+ and live cells by plotting forward scatter area versus Ghost viability dye. Single cells were selected by plotting side scatter height versus side scatter area. CD11b+ were plotting by count versus CD11b area. Immune cells were gated as follows in tumor isolated: Macrophages: (CD11b+ F4/80+); M1-like TAM (CD11b+, F4/80+ Ly6G- Ly6C-low/- MHCII-high); M2-like TAM (CD11b+ F4/80+ + Ly6G- Ly6C-low/- MHCII-low); dendritic cells (F4/80- Ly6C- CD11c+ MHCII+). CD3+ T cells (CD11b- CD3+) (CD3+ cells were confirmed by back gating with CD4+), CD4+ T cells (CD11b- CD3+ CD4+, CD8-), and CD8+ T cells (CD11b- CD3+ CD4-, CD8+). Relates to Figures 2 and 3. (**B**) Bone marrow and spleen single cell suspension are isolated as the following. After gating total cells by plotting forward scatter versus side scatter areas, single cells by plotting side scatter height versus side scatter area, and live cells by plotting side scatter area versus Ghost viability dye, immune cells were gated as follows: Total MDSC (CD11b+ Gr-1+); M-MDSC (CD11b+ Gr-1+ Ly6C-high Ly6G-); PMN-MDSC (CD11b+ Gr-1+ Ly6C-low Ly6G+); Macrophages: (CD11b+ Gr-1- F4/80+); M1-like macrophages (CD11b+ Gr-1-F4/80+ MHCII-high); M2-like macrophages (CD11b+ Gr-1-F4/80+ MHCII-low/-); dendritic cells (DC, F4/80- Ly6C- CD11c+ MHCII+). Relates to Figure 4 and 5.

A

Genes upregulated by anti-PD-1			
Gene	Log Fold Change	IgG2a (median)	anti-PD1 (median)
Ier3	0.95	7.82	8.30
Mt1	0.77	7.95	8.33
Mt2	0.76	7.51	7.88
Cks1b	0.65	6.94	7.27
Nxf1	0.64	6.85	7.17
Rbm8a	0.64	6.95	7.27
Mif	0.57	8.97	9.25
Ccl7	0.56	7.60	7.89
Ube2c	0.56	7.48	7.76
Nhp2	0.54	7.44	7.71
Tuba1c	0.52	9.09	9.35
Mcm3	0.52	7.46	7.72
Emg1	0.52	6.84	7.10
Rps27a	0.52	9.98	10.23
S100a6	0.52	10.55	10.81
Rpl22	0.51	8.44	8.70
Rpl36a	0.51	9.06	9.31
Ccl2	0.51	7.48	7.73
Srsf3	0.51	8.40	8.65
Aprt	0.51	8.19	8.45
Ppid	0.50	7.58	7.83

B

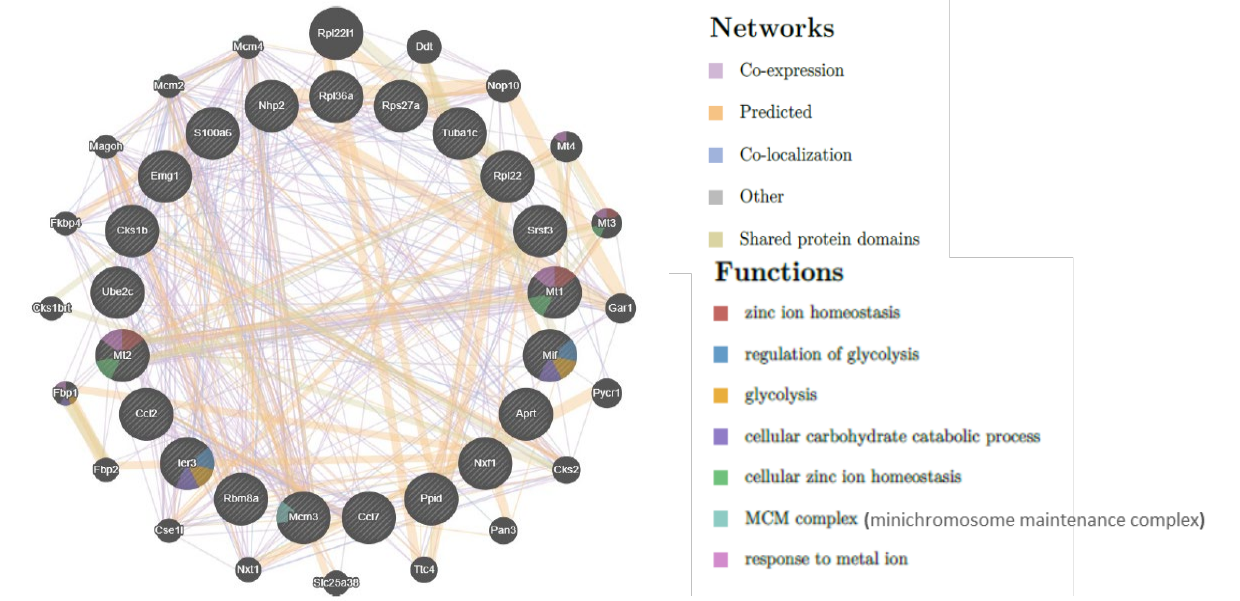

C

Genes downregulated by anti-PD-1			
Gene	Log Fold Change	IgG2a (median)	anti-PD1 (median)
Adipor2	-0.50	7.11	6.85
Acadm	-0.52	6.33	6.07
Ifi207	-0.53	6.04	5.77
Tln2	-0.54	6.40	6.13
Sbf2	-0.54	6.00	5.73
Mfn2	-0.54	6.40	6.13
Lpgat1	-0.55	7.40	7.13
Ehd4	-0.55	7.77	7.49
Rnf31	-0.57	6.14	5.85
Lamb2	-0.57	6.33	6.05
Tln1	-0.57	9.41	9.12
Rgp1	-0.58	5.09	4.80
Nrros	-0.58	6.08	5.79
Rps6ka3	-0.58	5.30	5.01
Vsir	-0.58	7.35	7.06
Acox1	-0.59	6.08	5.79
Akap2	-0.60	7.51	7.22
Card10	-0.61	5.60	5.30
Utrn	-0.63	6.72	6.40
Cped1	-0.64	5.57	5.25
Tnrc18	-0.64	6.98	6.66
Lnpep	-0.65	6.54	6.21
Wdfy3	-0.65	6.30	5.97
Rassf8	-0.66	6.25	5.93
Pkd1	-0.68	6.62	6.28
Aqp1	-0.68	7.51	7.17
Kat2b	-0.70	5.68	5.33
Fblim1	-0.71	5.63	5.27
Dhrs9	-0.71	5.50	5.14
Srcap	-0.72	5.98	5.62
Il6st	-0.72	7.05	6.69
Shank3	-0.73	6.02	5.65
Zfp106	-0.74	8.27	7.90
Zbtb4	-0.76	5.29	4.92
2900097C1	-0.77	5.76	5.37
Pnpla2	-0.77	6.47	6.08
Wdfy4	-0.77	5.33	4.94
Notch1	-0.78	7.05	6.66
Nsf	-0.78	6.76	6.37
Mga	-0.78	5.84	5.45
Prr14l	-0.79	5.17	4.78
Gse1	-0.80	5.82	5.42
Slc39a10	-0.85	6.72	6.30
Tenm4	-0.95	7.36	6.89
Tns1	-0.98	7.54	7.05
Siglec1	-1.12	5.91	5.36
Ralgapb	-1.22	5.41	4.81

D

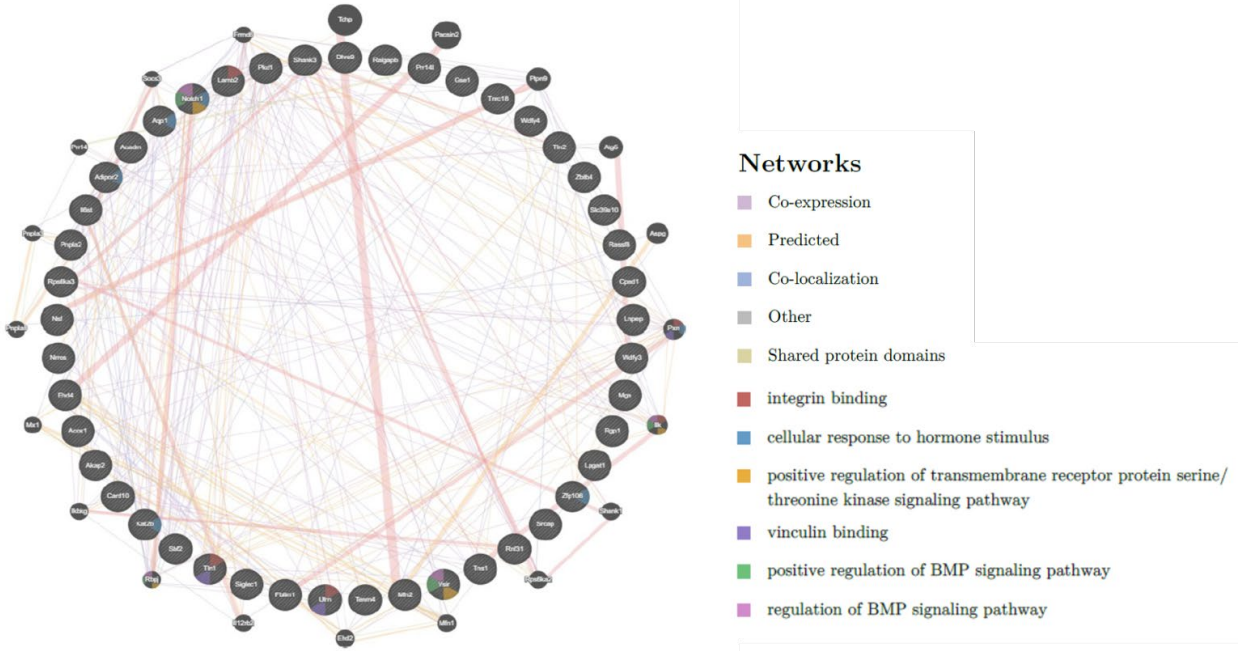

Supplemental Figure 3. Network analysis of up- and down-regulated genes in tumors from obese mice treated with control or anti-PD-1 antibody. A. List of genes that are upregulated with treatment with anti PD-1 compared to IgG2a. **B.** Network analysis of upregulated genes in obese mice tumors treated with control or anti-PD-1 antibody using GeneMANIA. Relates to Figure 3. **C.** List of genes that are downregulated with treatment with anti PD-1 compared to IgG2a. **D.** Network analysis of downregulated genes in obese mice tumors treated with control or anti-PD-1 antibody using GeneMANIA. Relates to Figure 3.

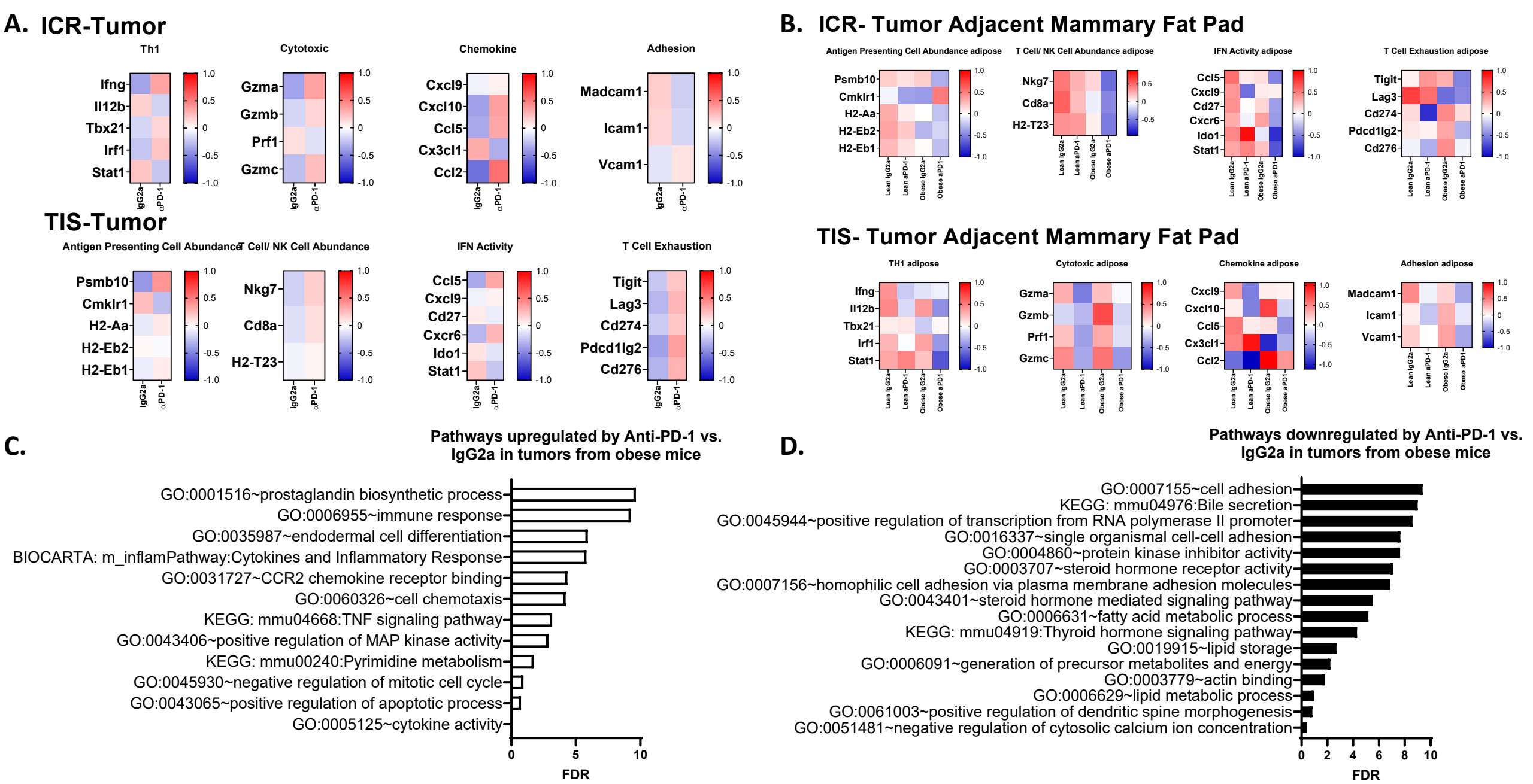

Supplemental Figure 4. Pathways regulated in tumors from obese mice treated with control or anti-PD-1 antibody demonstrate reprogramming of TME. A. Immunologic Constant of Rejection (ICR) and Tumor Inflammation Signature (TIS) in the obese tumor in mice treated with IgG2a and PD-1. **B.** ICR and TIS in lean and obese tumor adjacent mammary fat pad. **C-D.** DAVID analysis was used to generate pathways upregulated (C) or downregulated (D) by anti-PD-1 compared to IgG2a (FDR, false discovery rate). Relates to Figure 3.

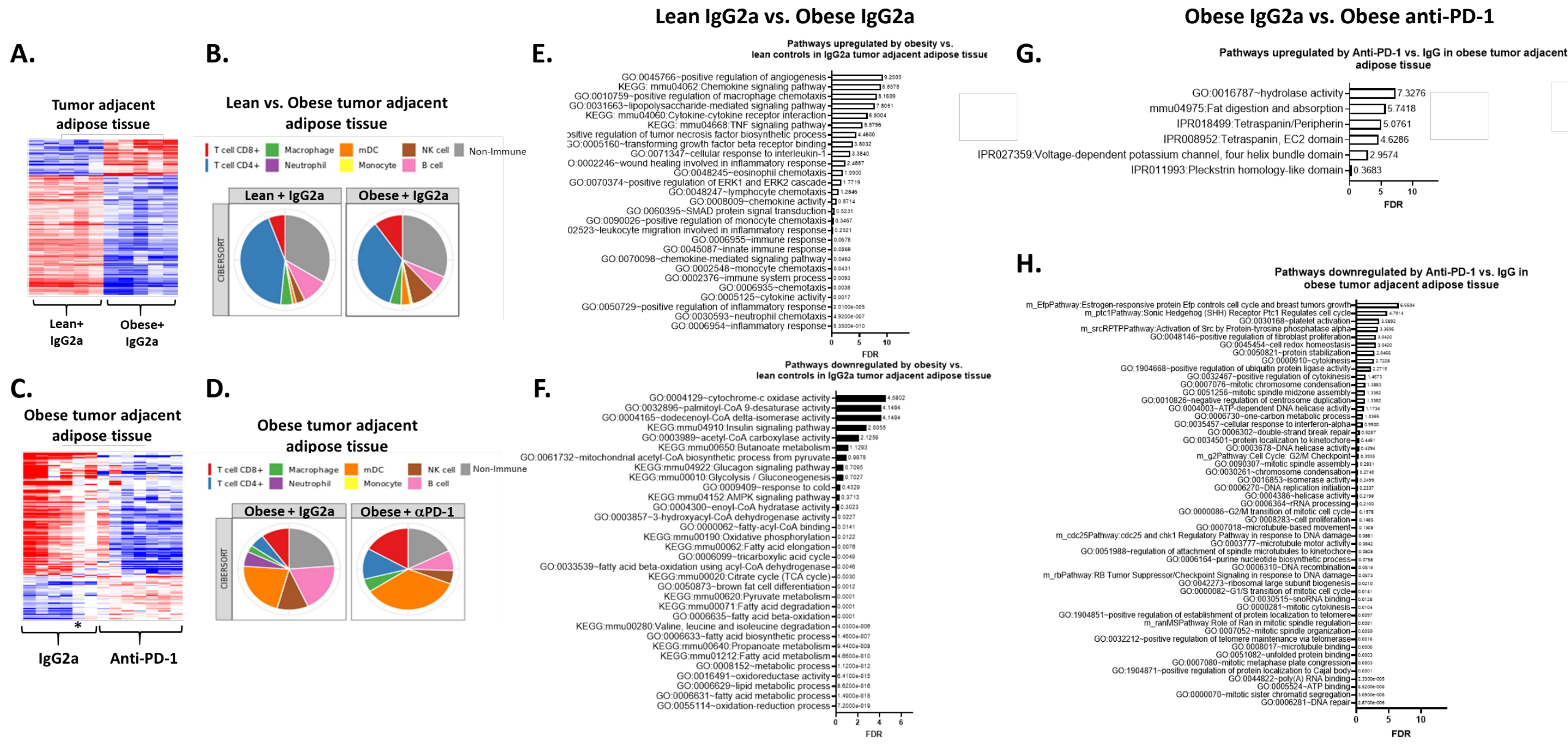

Supplemental Figure 5. Anti PD-1 treatment is more effective in obese compared to lean mice with significant impacts on immune cell infiltration in tumor adjacent adipose tissue. A. Heat map showing RNA-seq normalized gene expression values (N=200) in the tumor adjacent adipose tissue of lean and obese mice treated with IgG2a (n=5) and anti-PD-1 antibody(n=5) (SigClust P=0.001). **B.** Pie chart of immune infiltration in tumor adjacent adipose tissue of obese and lean mice treated with IgG2a antibody generated using CIBERSORT. **C.** Heat map showing RNA-seq normalized gene expression values (N=150) in the tumor adjacent adipose tissue of obese mice treated with IgG2a (n=5) and anti PD-1 antibody (n=8, *indicates 1 sample misclassified). **C.** Pie chart of immune infiltration in tumor adjacent adipose tissue of obese mice treated with IgG2a and anti-PD-1 antibody generated using CIBERSORT. **E-F.** DAVID analysis was used to generate pathways upregulated (E) or downregulated (F) by obesity compared to lean mice, both treated with IgG2a control isotype antibody. **G-F.** DAVID analysis was used to generate pathways upregulated (G) or downregulated (H) by IBC in obese mice treated with anti-PD-1 compared to obese mice treated with IgG2a control isotype antibody (FDR, false discovery rate). Relates to Figure 3.

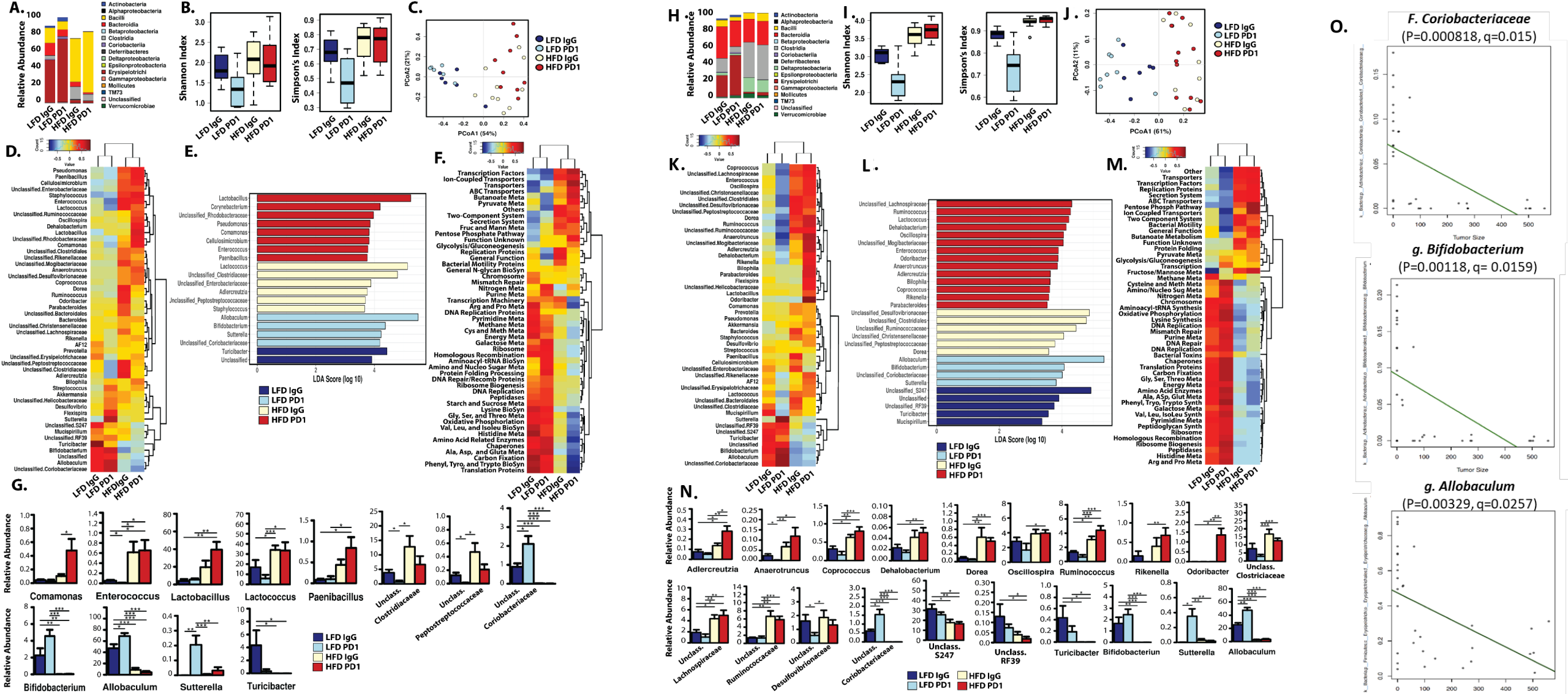

Supplemental Figure 6. The jejunum microbiome is impacted by diet and anti-PD-L1 immunotherapy. Jejunal (**A-G**) or cecal (**H-N**) contents were isolated from tumor-bearing mice at sacrifice from obese (HFD) or Lean (LFD) fed groups. Mice had E0771 tumors treated with IgG2a control or anti-PD-1 as above. **A,H.** Relative abundance of taxonomic composition at the class level. **B,I**. Alpha diversity by Shannon and Simpson's indexes. **C,J**. Beta diversity displayed was calculated by Bray Curtis and displayed as principal coordinate analysis (PCoA). Permutational multivariate analysis of variance in jejunum (PERMANOVA) R2 = 0.521, P = 0.0003; PERMDISP2 P = 0.0013 and in cecum (PERMANOVA) R2 = 0.567, P = 0.0003; PERMDISP2 P = 0.0015. **D,K**. Heatmap of the 50 most abundant microbial taxa as calculated by Spearman's rank correlation coefficient. **E,L**. Linear discriminant analysis (LDA) effect size (LEfSe) by genus. **F,M**. Heatmap of the 50 most abundant phylogenetic Investigation of Communities by Reconstruction of Unobserved States (PICRUSt) predicted metabolic pathways calculated by Spearman's rank correlation coefficient. **G,N**. Select graphs of taxa with significantly demonstrated changes between treatment groups IgG and anti-PD-1 immunotherapy in the jejunal or cecal contents. * P<0.05, ** P<0.01, ***P<0.001 by 2-way ANOVA. Mean -/+ SEM of relative abundance shown. N=6-10, Je, N=6-11 Je. **O.** Correlations of cecal microbial taxa with tumor volume at endpoint using Multivariate Analysis by Linear Models (MaAsLin) for F. *Coriobacteriaceae* (P=0.000818, q=0.015), *g. Bifidobacterium* (P=0.00118, q= 0.0159), and *g. Allobaculum* (P=0.00329, q=0.0257) are shown. Relates to Figure 6.